High-speed, high-resolution fiber Bragg grating matrix structural health monitoring system

Kelvin Chau[a], Pizhong Qiao[b], Wayhu Lestari[b], Richard J Black*[a], Behzad Moslehi[a]
[a]Intelligent Fiber Optic Systems Corporation, 2363 Calle Del Mundo, Santa Clara CA 95054-1008
[b]Washington State University, Dept. of Civil & Environmental Eng., Pullman, WA 99164-2910

ABSTRACT

Structural Health Monitoring (SHM) is becoming an increasingly important tool for the maintenance, safety and integrity of aerospace structural systems. Immune to electromagnetic interference, Fiber Bragg Grating (FBG) optical sensor matrices are light-weight and multiplexable, allowing many sensors on a single fiber to be integrated into smart structures. Highly sensitive to minute strains, they can facilitate maximum SHM functionality, with minimum weight and size. Consequently, these optical systems, in conjunction with advanced damage characterization algorithms, are expected to play an increasing role in extending the life and reducing costs of new generations of structures and airframes. In this paper, we discuss the development of both hardware and algorithms to detect, locate and quantify delamination in composite laminated beam structures. We present an integrated SHM system including (a) the capability of interrogating over 50 FBG sensors simultaneously with sub-picometer resolution at over 50 kHz, (b) an FBG-sensor/piezo-actuator matrix smart skin design and methodology, and (c) damage detection location and quantification algorithms based on mode shape or other relevant advanced algorithmic-based damage diagnosis and prognosis techniques. Comparison with other SHM systems (e.g., based on piezo-electric (PVDF) and Scanning Laser Vibrometer sensors) demonstrates better signal-to-noise and damage detection for our FBG system.

Keywords: Fiber optics, optical fiber sensors, fiber gratings, structural health monitoring, high-temperature sensors

1 INTRODUCTION

Structural health monitoring (SHM) is becoming increasingly important in the maintenance of safety and integrity of aerospace structural systems, and has significant potential in both future space exploration missions and in air transportation security. A robust and reliable nondestructive damage identification and assessment capability in such a monitoring system is essential to predictable maintenance and disaster avoidance. Undetected or untreated, damage may grow and lead to catastrophic structural failure. Damage can occur in many different forms, such as fatigue cracks, corrosion and dents in metals; delamination, disbonding and fiber breakage in composites; impact and battle damage. These damages can be originated from the strain/stress history of the material, imperfections or tooling impact in the manufacturing process. Damage can likewise develop during service life as wear and tear or under extraordinary circumstances, such as temperature cycling, impact of flying objects or ballistic impact in the battlefield. Early detection or monitoring is the key to preventing a catastrophic failure of structures, especially when these are expected to perform near their limit conditions. The increasing cost associated with maintaining and servicing structures has driven commercial and defense industries to look into methods for accurately assessing the presence and extent of damage in a system. Manufacturers as well as maintenance personnel have great needs significantly to improve safety and reliability while achieving lower inspection and maintenance costs.

Development of a reliable monitoring system will prove a key part of future structural preventive maintenance programs, thus ensuring the safety and integrity of material, components and systems, ultimately enhancing the life of structures and the affordability of structural systems over their lifetime. The ultimate goal of SHM technology is development of autonomous systems for continuous monitoring, inspection and damage detection of structures with minimum labor involvement. The monitoring system will regularly acquire and analyze the response data, preferably while the structure is in service, and indicate the damage, as graphically illustrated in Figure 1. Conventional Non-Destructive Evaluation (NDE) techniques are deployed within the framework of SHM. However, despite newer developments in the fields of computer science and technology enhancing the capability and efficiency of these detection methods, it is still difficult to implement advanced methods for on-board, automatic, real-time, global health monitoring of aerospace structures. The

difficulties and complexities involved motivate many researchers to develop alternative methods and systems to detect the existence of damages in a structure in order to evaluate the condition of that structure.

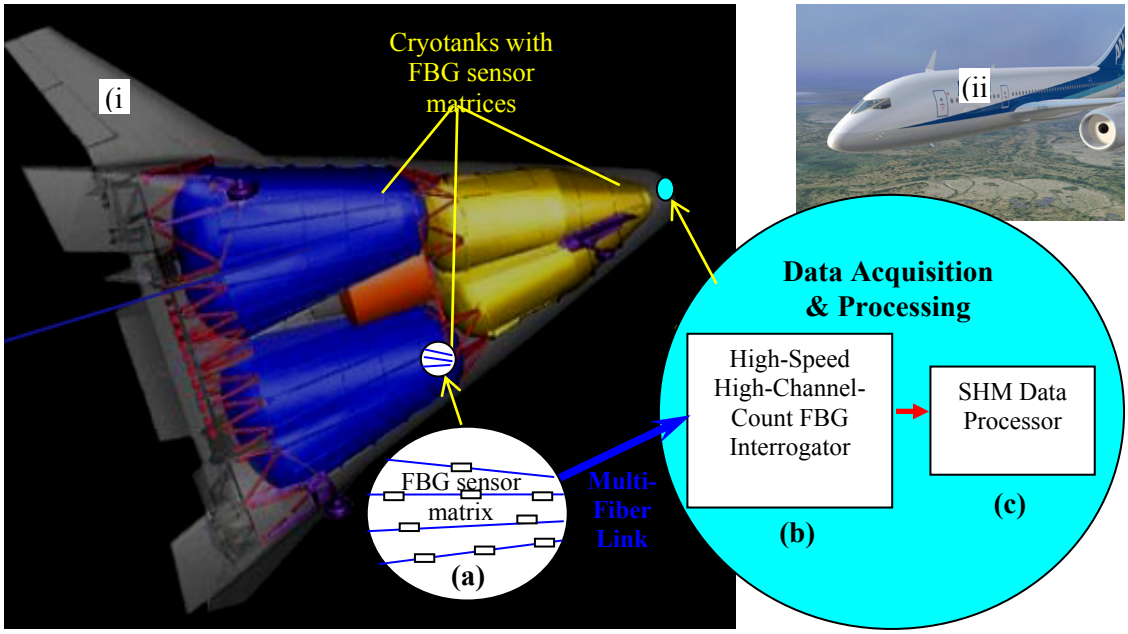

Fig. 1. IFOS vision of Structural Health Monitoring (SHM) for (i) aerospace systems involving cryogenic fuel tanks and (ii) future commercial aircraft with matrix arrays of Fiber Bragg Grating (FBG) sensors (a) on the cryogenic tanks or wings and fuselage feeding data to an on-board data acquisition and processing system incorporating a powerful parallel processing FBG interrogator (b) and a SHM data processor (c).

2 FIBER BRAGG GRATINGS (FBGS) FOR SHM

Fiber Bragg Gratings have been established as an important sensor component for strain measurements in smart structures. This is chiefly due to their precision, resolution and reliability, tolerance of extreme conditions and immunity to RF electromagnetic interference. In many applications, arrays of FBG sensors along a single fiber at multiple locations are required to collect data samples at high speed with micro-strain resolution. However, traditional approaches to processing the optical signals may be either lacking in sampling rate speed or are cost-prohibitive, as the number of optical sensors increases. One of the recent objectives of Intelligent Fiber Optic Systems Corporation (IFOS) has been to identify an interrogation technique that is most suitable for supporting a larger number of FBG sensors (several hundred per fiber) at high speed (several MHz).

The basic principle of a Fiber Bragg grating (FBG)-based system lies in the resonant frequency of the FBG. The Bragg wavelength is related to the refractive index of the material and the grating pitch. The spectral width defined by the passband of such a grating forms a channel, which will reflect a characteristic wavelength, allowing the remainder of the spectrum to go through with insignificant optical loss, as shown schematically in Fig. 2. FBGs thus operate by acting as a wavelength selective filter that reflects a single wavelength, called the Bragg wavelength, λ_B. The Bragg wavelength is related to the grating pitch, Λ, and the mean refractive index of the core, n, by $\lambda_B = 2\Lambda n$. Both the fiber refractive index (n) and the grating pitch (Λ) vary with changes in pitch or temperature.

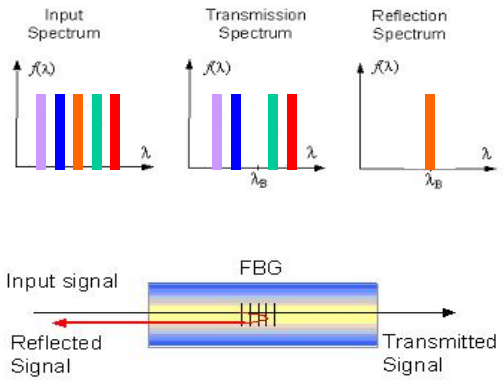

Fig. 2. Functional principle of a fiber optic Bragg grating.

Fiber Bragg Grating (FBG) sensing systems are being deployed in a wide variety of applications for structural health monitoring. The potential of fiber optic sensors to deliver new and effective measurement in many applications is becoming clear. Development of such Fiber Optic Sensor (FOS) technology has been increased vastly, leading to many novel applications in various structures. Sensing capacities of the FOS's, which include the ones to obtain information easily and process the information efficiently, determine the success of their applications. Advantages of fiber Bragg grating (FBG) based sensor have motivated implementation in the area of structural monitoring applications, such as monitoring or measuring strain, fracture, vibration or simultaneously sensing multiple parameters 1. These optical sensors are immune to electromagnetic interference (EMI) and hence exceptionally suitable to applications where EMI is a concern. Moreover, these sensors are available in various sizes and can be conveniently embedded to the host structures without causing mechanical disturbances or defects. The ability of FBG sensors simultaneously to measure multiple locations, due to its wavelength division multiplexing capability, attracts much interests for research and development in the implementation of FBG sensors for damage detection and structural health monitoring 1-6.

3 DAMAGE DETECTION

Dynamic response-based damage detection offers a simple identification method with easy implementation. The basic assumptions of this technique are that the dynamic parameters such as natural frequencies, mode shapes, transfer functions, or response functions are themselves functions of the physical properties of the structures. Therefore, the changes in these dynamic characteristics can be used to locate and assess localized physical and structural damage.

Vibration-based nondestructive evaluation is among the most common methods used to characterize damage in a structure. The underlying premise behind vibration based Non-Destructive Testing (NDT) techniques is to excite the structure and then monitor its resulting vibration characteristics to characterize the damage. The excitation forces the defect to open and close thereby allowing for easier detection as the structure transitions between these two states as opposed to continually being closed or open. Damage causes variation in the material properties (i.e., mass and/or stiffness), which in turn causes the natural frequencies of vibration to change. By comparing the current vibration response to that of a baseline "healthy" structure, it is possible to detect the presence of damage. The combination using of fiber optic sensing and piezoceramic actuation for simultaneous impedance-based structural health monitoring and vibration suppression has been presented in the literature 9-13. FBG sensing technology based on a built-in network of piezoelectric actuators and sensors are viable and cost-effective means of monitoring the structure condition and detecting damage while the structures are in service 7-8. The hybrid system can be used to perform quick non-destructive evaluation and long-term health monitoring of aerospace vehicles and structures. The health monitoring system combines structurally integrated sensor network, signal processing instrumentation, and data interpretation software to allow real-time in-situ monitoring, early detection, and long term tracking of structural damages 14. With this system, the emerging concept of structural health monitoring can become a commercially viable option in structural engineering, allowing a new generation of safer, more reliable, and lower maintenance structures. The developed structural diagnostic system can permit quantitative characterization and event determination pertaining to aerospace

structures in hostile service environments. More specifically, the hybrid system can potentially be used to perform, 1) In-situ material property characterization, 2) Detect material and structural defects, 3) Detect damage including corrosion, 4) Characterize load environments (fatigue, overload).

The procedure for damage assessment is summarized in a diagram presented in Fig. 3.

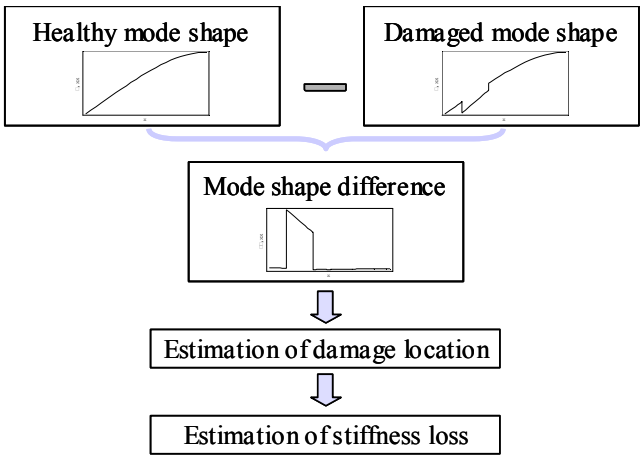

Fig. 3. Damage detection procedure.

We refer to [18] for details. The key points are as follows:- When damage is introduced in a structure, the bending stiffness at the location of the damage is reduced while at the same time the magnitude of the curvature modes increases. The absolute differences between the curvature modes of the intact and damaged structures are the highest in the region of the damage and negligibly small outside this region. Hence, the absolute curvature difference between the healthy and damaged structures for each mode can be used to identify damage location and represented as:

$$\Delta\phi''^{2}_{\mathrm{i,j}} = \left| \left\{\phi''_{\mathrm{h}}\right\}^{2}_{\mathrm{i,j}} - \left\{\phi''_{\mathrm{d}}\right\}^{2}_{\mathrm{i,j}} \right| \tag{1a}$$

$$\boldsymbol{D}_{\mathrm{j}} = \sum_{\mathrm{i}} \Delta\phi''^{2}_{\mathrm{i,j}} \tag{1b}$$

where ϕ''_i or $\phi_{i,xx}$ is the i^{th} curvature mode shapes; *h* and *d* denote healthy and damaged, respectively; and *i* and *j* denote the mode number and the measurement location, respectively. The curvature damage factor (CDF), D_j, is the summation of damage differences from each mode being evaluated. Based on the curvature difference values and CDFs, the location of damage in the structure can be identified.

Once the damage is identified, for example at location x_d, the magnitude of the damage at this location can be defined by using the damage magnitude difference of the modes, $\Delta\phi_{i,xx}(x_d)$, between the intact structure and the structure with damage. This damage magnitude or stiffness loss ε can be calculated using results in [18]. Since the frequency measurements at low frequency are sensitive to interferences, the damage magnitude prediction is calculated based on the curvature mode shape relationship. Provided the damage location x_d is established, the damage magnitude in the form of stiffness loss can be defined as follows

$$\varepsilon = \frac{\phi_{i,xx} - \phi_{id,xx}}{\sum_{j=1}^{n} \frac{\lambda_i^0}{\lambda_i^0 - \lambda_j^0} \left\{G_{1\mathrm{j}} - G_{2\mathrm{j}} + G_{3\mathrm{j}} - G_{4\mathrm{j}} - G_{5\mathrm{j}}\right\} \frac{d^2}{dx^2}\phi_j^0 - \left[\mathbf{H}(x-x_1) - \mathbf{H}(x-x_2)\right] \frac{d^2}{dx^2}\phi_i^0(x)} \tag{2}$$

where $\phi_{i,xx}$ and $\phi_{di,xx}$ are the measured curvature modes of the healthy and damaged beams at the i^{th} mode, respectively.

In some cases such as structures that are already in service for long period, data of healthy or undamaged structures are rarely available. These healthy data can be approximated by using a gapped-smoothing technique, where the basic assumption of the technique is that a mode shape of a healthy structure has a smooth surface **19**. Using the mode shape

data of damaged structure and interpolation technique with polynomial approximation, the smooth mode shape surfaces of healthy structure are estimated. For the beam structures, the undamaged curvature is approximated by using a variable polynomial to gap-smooth fit the measured data

$$U_{GSM}(x) = \phi_h^{"} = \sum_{i=0}^{n} C_i X^i \tag{3}$$

where the C_j is the coefficients calculated by using curve-fitting.

4 EXPERIMENTAL STUDY

The experimental study includes specimen preparation (i.e., specimen manufacturing and sensor placement), vibration testing set-up and dynamic response measurement.

4.1 Specimen Preparation

The composite specimen used in this study was fabricated using vacuum bagging process. It was made of E-glass fiber and epoxy resins and has a $[CSM/0(90/0)_3]_S$ lay-up for a total of 16 layers as shown in Fig. 4. UM 1208 (CSM + Unidirectional) stitched combo layer has a thickness of approximately 0.49 mm (0.0189 in.) for unidirectional ply and 0.23 mm (0.0087 in.) for CSM ply. The thickness of C1800 is 0.28 mm/ply (0.0117 in.) and 0.56 mm/mat (0.0220 in.). The 16 layers lead to a total composite thickness of 4.8 mm (0.189 in.). A composite plate was first fabricated, and it is later cut into several beam samples with dimensions of 0.0508 m (2 in.) wide and 0.6096 m (24 in.) long as shown in Fig. 5. The length of the beam for cantilevered condition is 0.5588 m (22 in.). Fig. 6 shows the picture of the beam specimen with delamination.

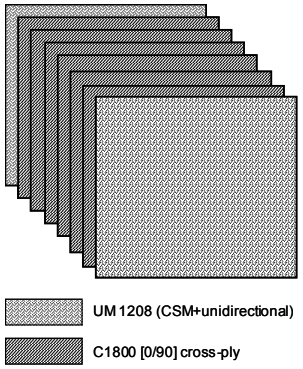

Fig. 4. Lay-up of composite samples.

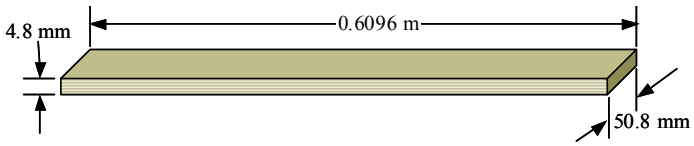

Fig. 5. Dimension of beam specimens.

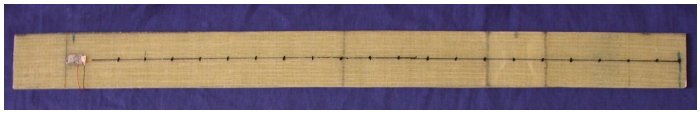

Fig. 6. Beam sample with delamination.

A defect or damage in the form of delamination is used to demonstrate the proposed health monitoring method. The delamination was introduced in the beam by inserting a Teflon film between the second and third layer of the composite laminate during the manufacturing process. After the curing, the Teflon film is pulled out leaving a debonded area (delamination) in the beam sample between the second and third layers. In this study, the delamination is approximately 50.8 mm (2 in.) in length located at 0.3810 m (15 in.) from the cantilevered end.

The FBG sensors are bonded carefully to the composite beam using epoxy glue at 16 FBG measurement locations with equal distance (see Fig. 7b). The delamination is located between the sensors 11 and 13, with sensor 12 is in the middle of delamination. The shrinkage of the sensors after bonding is examined to ensure that the wavelength of each sensor after bonding does not fall out of the wavelength range of the interrogation module. The wavelength of each sensor is calibrated before the bonding and then is measured again after the epoxy completely cured and dry. Comparison between the wavelength measurements of before and after bonding shows that the shrinkage of the sensors due to bonding only causes shift of the wavelength less than 1 nm. Hence, the measured signals are still in the range of the interrogation module and do not cause saturation.

4.2 Experimental Set-up and Measurement

The beam specimen is tested in a cantilevered configuration (see Fig. 7a)). The vibration testing is performed to measure the strain distribution of the beam structure, from which the curvature shapes are constructed. The time domain data from the FBG interrogation system is subsequently transformed and processed to obtain the frequencies and mode shapes of the cantilever beam. The beam is excited by using a PZT actuator for up to 400 Hz (Fig. 7c)) to capture the first four mode shapes. Then, the measured time domain data are transformed to frequency domain data using MATLAB routine and prepared in the format suitable for the ME'scope modal analysis software. The obtained frequencies and frequency response functions from FBG system are then compared with the measurement results using other sensor systems, i.e., the piezoelectric (PVDF) films (which are also strain-based measurement sensors) and the displacement-based scanning laser vibrometer (SLV) system.

(a) Cantilevered composite beam

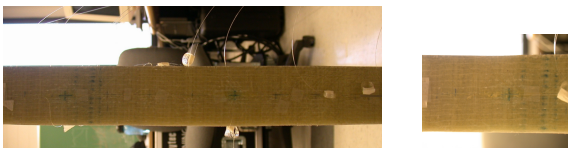

(b) FBG sensors bonded to the surface of the beam

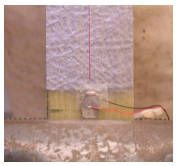

(c) PZT actuator bonded at the root of the beam

Fig. 7. Picture of composite beam with installed FBG sensors and PZT actuator

Preliminary results of the experimental measurement and comparison with other sensor systems demonstrate the capability of the FBG sensors as a dynamic strain measurement device for structural health monitoring purpose. The first four modes of measured frequencies obtained from three different sensor systems are listed in Table 1. Comparison of the frequency response function (FRFs) obtained from the measured data are presented in Fig. 8. The measured frequencies and obtained FRFs from different sensors (i.e., FBG, PVDF and SLV systems) are very close and similar. The minor difference of frequencies in Table 1 may be caused by the clamping conditions in the cantilever beam, as it was installed at the different time for the three respective sensor systems. As shown in Fig. 8 at lower frequency, the FBG has better signal to noise ratio than the PVDF films due to the EMI insensitive property of the sensor. This advantage will be very useful for monitoring application where electrical interference may be significant. The FRF obtained from the FBG sensor and the corresponding coherence are also shown in Fig. 9, and the smooth FRFs indicates high signal to noise ratio (SNR) and good input/output coherence demonstrates the high resolution measurement of the FBG sensor and interrogation system.

Table 1 Measured natural frequencies from different sensors (first 4 modes).

Mode	Measured frequency, Hz		
	FBG	SLV	PVDF
1	9.16	9.38	7.81
2	57.34	58.13	54.69
3	162.6	165.1	168.8
4	312.4	316.7	320.3

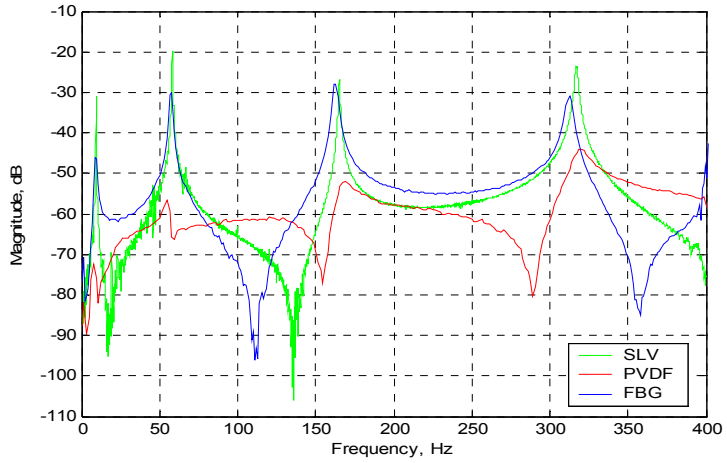

Fig. 8. Frequency response function comparison

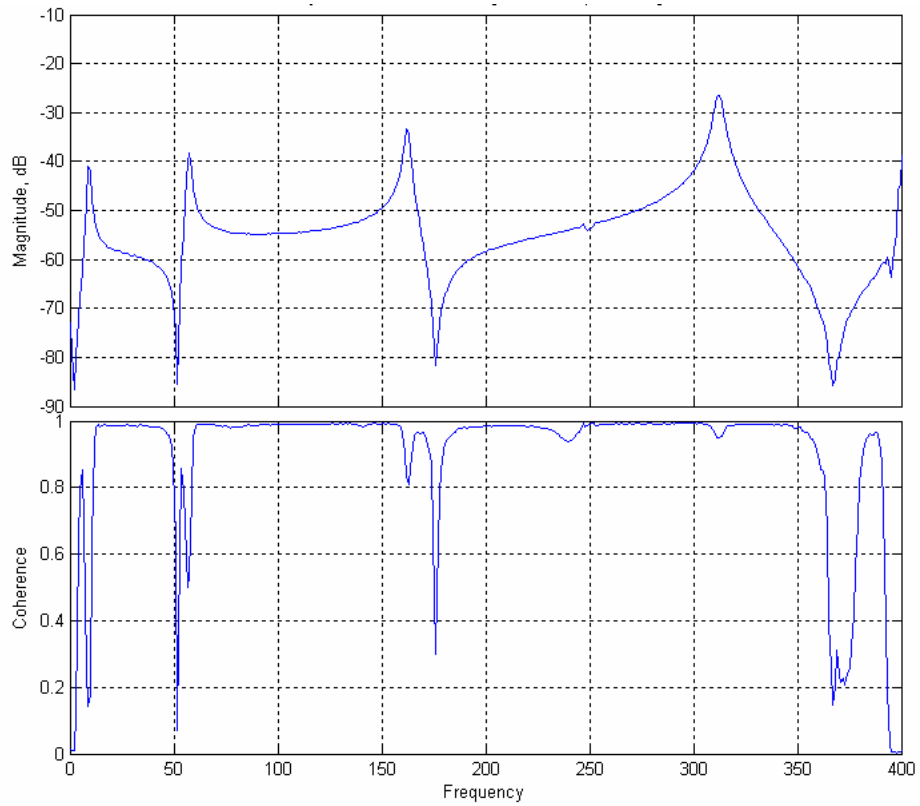

Fig. 9. Frequency response function from FBG and coherence.

4.3 Data processing and analysis

Data processing and analysis activity consists of two parts, i.e., modal analysis and data reduction to estimate location and quantity of damage based on the algorithm developed by two of the authors in [18].

4.3.1 Modal Analysis

After transformation into frequency domain data, the frequency response functions measured from each sensor were arranged into the input format for the ME'scope modal analysis. The obtained modal parameter, i.e., frequencies and curvature mode shapes, are presented in Table 2 and Fig. 10, respectively.

Table 2 Natural frequencies obtained from modal analysis

Mode	Frequency, Hz
1	9.16
2	57.34
3	162.55
4	312.43

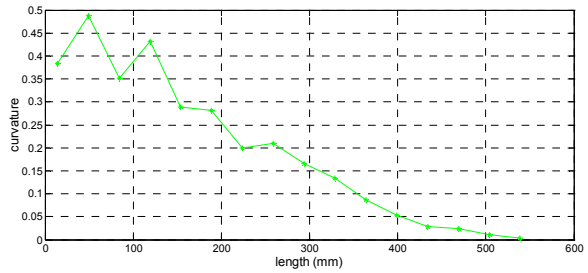

(a) first mode

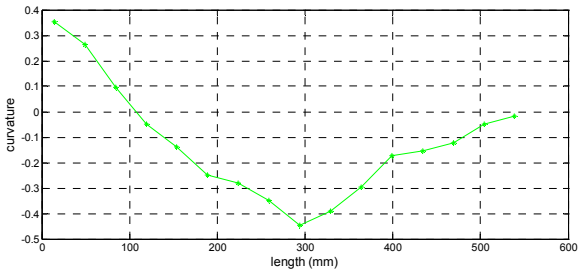

(b) second mode

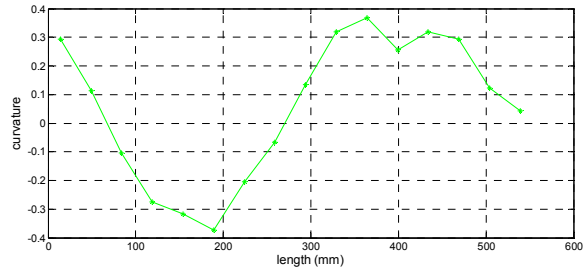

(c) third mode

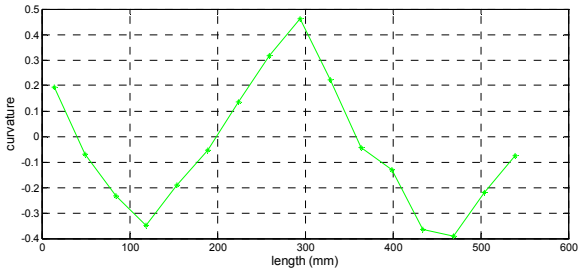

(d) fourth mode

Fig. 10. Curvature mode shapes of cantilevered composite beam from FBG data.

4.3.2 Damage Estimation

Curvature mode shapes of healthy/undamaged beam are estimated based on the measured curvature mode shapes presented in Fig. 10. Curvature mode shapes of cantilevered composite beam from FBG data.. Curvature damage differences of each mode and the curvature damage factor, D, are then calculated based on Eqs. 1(a) and 1(b), respectively. The results of estimated healthy curvature mode shapes are presented in Fig. 11 in comparison with the measured curvature mode shaped of damaged beam and along side the curvature damage differences of each mode are presented as well. Fig. 12 shows the curvature damage factor distribution along the beam length, computed using Eq. 1(b).

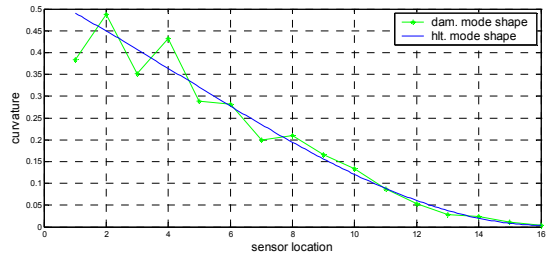

(a) the first curvature mode shapes

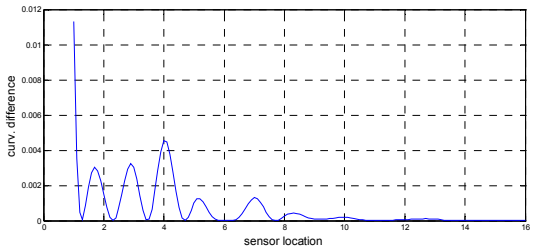

(b) curvature difference in the first mode

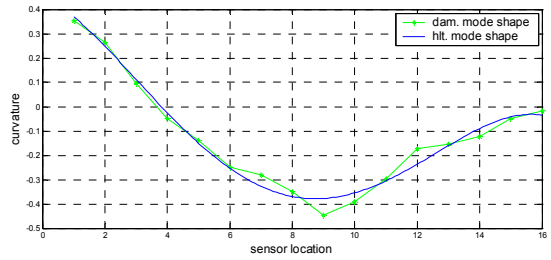

(c) the second curvature mode shapes

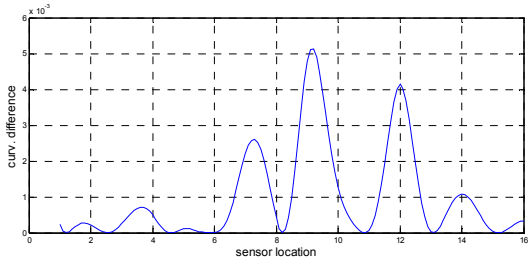

(d) curvature difference in the second mode

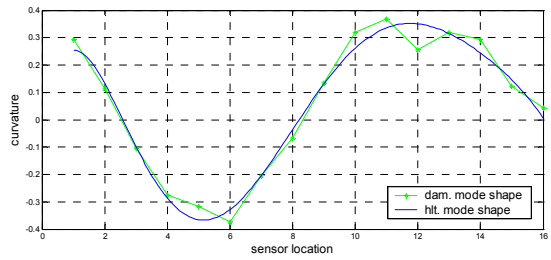

(e) the third curvature mode shapes

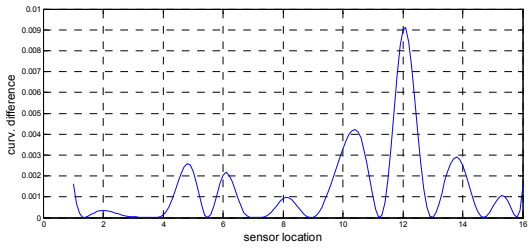

(f) curvature difference in the third mode

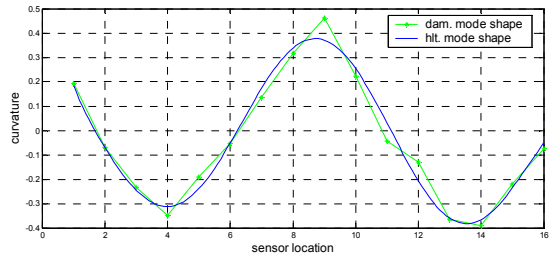

(g) the fourth curvature mode shapes

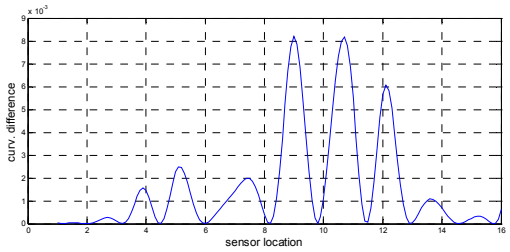

(h) curvature difference in the fourth mode

Fig. 11. Estimated healthy curvature mode shapes of cantilevered composite beam and curvature damage difference from FBG data.

Results for the first mode show a lot of undulation near the base of the beam; hence, it is not further considered in the calculation for identifying the damage. An obvious dent at the peak of the curvature wave of the third mode shapes (location 12) indicates possible location of damage in the beam Fig. 11e. This deduction is supported by the presence of significant variation in curvature mode shapes of the second and fourth modes. Consequently, the curvature difference from the three modes has a considerable value at location 12, especially from the third modes, where the location of the damage is at the peak of the curvature wave. However, a significant curvature difference of the fourth mode at location 9 may be misinterpreted as location of the damage as well. In this case, the curvature fitting process to estimate the healthy curvature mode shapes had difficulty to fit one wave that rise sharply more than the others. Ignoring this phenomenon in the curvature damage factor graph (Fig. 12), the damage location can be confidently identified between locations 11 and 12.

Once the damage location is identified using the curvature damage difference (see Fig. 11(f) of the third mode curvature shape or Fig. 12) of the curvature damage factor), the quantification of damage is calculated. The estimated stiffness losses at the area of damage are listed in Table 3. The estimation for stiffness loss is at best when the location of the damage is around the peak of the wave of the curvature mode shape, which in this case is the third mode (see Fig. 11(f)). Estimation based on the fourth mode produces very small stiffness loss due to the fact that the delamination is located near the nodal point. Hence, this estimation can be discarded. Thus, the stiffness loss of 21% (see Table 3) at sensor location 12 based on the third curvature mode shape (Fig. 10(e)) or curvature damage difference (Fig. 10(f)) can be regarded as a quantitative way of quantifying the delamination damage.

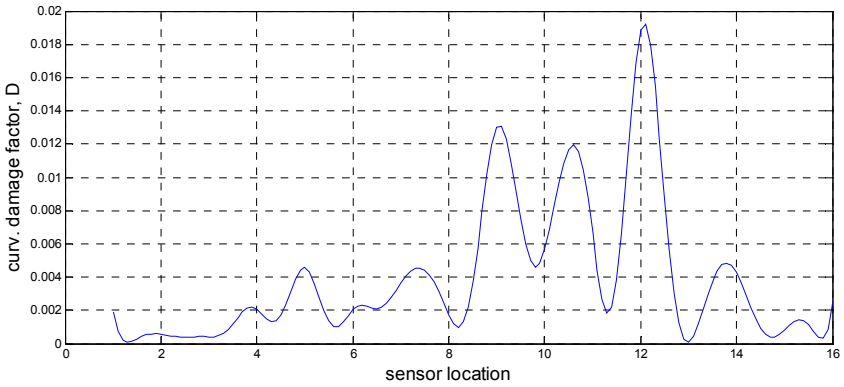

Fig. 12. Curvature damage factor

Table 3. Damage location and stiffness loss estimation.

Mode	Damage location	Stiffness loss, ε
1	n/a	n/a
2	12	5.6 %
3	**12**	**21 %**
4	11, 12	0.3 %

We have made very encouraging progress towards developing an effective and robust damage assessment technique using the high-speed Fiber-optic Bragg grating (FBG) interrogation system developed by IFOS, eventually evolving this to an on-line SHM system with particular emphasis on monitoring of aerospace structures. Qiao and Lestari had already established the potential of dynamics-based detection techniques using smart piezoelectric materials for identifying the presence and location of damage [2-3]. The challenge of utilizing the fiber-optic Bragg grating sensor system to measure dynamic response of the structures and establish the SHM algorithms is being investigated and addressed further. A combined experimental and analytical/numerical approach was used to develop the basis for a rapid and robust dynamics-based SHM system around IFOS' high-speed FBG interrogation systems.

5 CONCLUSIONS

In the work reported in this paper, we successfully developed and implemented the laboratory setup and demonstrated the feasibility of an effective and robust damage assessment technique using a high-speed FBG interrogation system developed by IFOS. In parallel, IFOS has investigated interrogation techniques based on scanning (AOTF) and parallel

processing (AWGs), and concluded that the approach using parallel processing has more potential for SHM applications. Parallel processing can provide simultaneous measurements from a large number of sensors along a single fiber. The simultaneity preserves phase relationship among sensors (an important factor in the wave arrival algorithmic analysis of defect location and size), which the tunable approach cannot accomplish. This approach could extend our damage assessment technique to much higher speeds (several MHz) and potentially allow us to construct an interrogator system to support more than 800 FBG sensors in a single fiber using Wavelength Division Multiplexing (WDM). With *N* fibers, matrix arrays of 800 x *N* sensors could be addressed.

We found that FBG sensors are superior to their electronic counterparts for the application and demonstrated our photonic parallel spectral processor interrogator, capable of sub-picometer measurand-induced (strain etc.) wavelength shifts at high speeds (5 kHz). Measured data from vibration testing with FBG sensors shows very good agreement with the results based on other sensor systems (i.e., PVDF and SLV). At low frequency, the FBG has better signal to noise ratio (SNR) than the PVDF films due to the EMI insensitive nature of the sensor. This advantage will be very useful for monitoring application where the presence of electrical interference is significant, such as within a radome space. Compared to the displacement-based SLV measurement, the strains acquired from the surface bonded FBG sensors can be directly treated as curvatures of vibrated beams, thus eliminating the further data reduction from the displacement mode shapes and offering the simplicity of damage detection approach.

The quality of the measured data from each sensor is very important for successful damage estimation. While the FBG sensors in general have high SNR, good synchronization in recording the excitation and measured signal of each sensor are essential to produce reliable modal analysis results.

A damage detection procedure has been developed, implemented and validated initially in the context of a 1D structure. The damage location is confidently estimated based on obtained curvature mode shapes. The best estimation of stiffness loss is achieved by using the curvature mode shapes, which have a wave peak at the location of the damage. In this case, it is the third curvature mode shape.

In summary, the FBG sensor matrices (in this preliminary work as a line of 16 FBG sensors) together with the IFOS interrogation system provide high resolution measurements of dynamic response (e.g., FRFs and curvature mode shapes), and in combination with the proposed active perturbation-based damage detection technique, the system successfully locates and quantifies the delamination damage in the composite sample. It demonstrates that the FBG-measured curvature mode shapes can be used as an effective and valid approach to locate and quantify the damage in composite structures.

ACKNOWLEDGEMENTS

We thank Dr. R.S. Rogowski of NASA for helpful comments, and NASA Langley Research Center for support.

REFERENCES

1. Tennyson, R.C., Mufti, A.A., Rizkalla, S., Tadros, G., Benmokrane, B., 2001, Structural health monitoring of innovative bridges in Canada with fiber optic sensors, *Smart Mater. Struct.* **10**, 560–573.
2. Chan, T.H.T., Yua, L., Tam, H.Y., Ni, Y.Q., Liu, S.Y., Chung, W.H., Cheng, L.K., 2006, Fiber Bragg grating sensors for structural health monitoring of Tsing Ma bridge: Background and experimental observation, *Engineering Structures* **28** 648–659.
3. Takeda, N., Okabe, Y., Kuwahara, J., Kojima, S., and Ogisu, T., 2005, Development of smart composite structures with small-diameter fiber Bragg grating sensors for damage detection: Quantitative evaluation of delamination length in CFRP laminates using Lamb wave sensing, *Composites Science and Technology* **65** 2575–2587.
4. Yang, Y.C. and Han, K.S., 2002, Damage monitoring and impact detection using optical fiber vibration sensors, Smart Mater. Struct. 11 337-345.
5. Todd, M.D., Johnson, G.A. and Vohra, S.T., 2001, Deployment of a fiber Bragg grating-based measurement system in a structural health monitoring application, *Smart Mater. Struct.* **10** 534–539.
6. Ling, H.Y., Lau, K.T. and Cheng, L., 2004, Determination of dynamic strain profile and delamination detection of composite structures using embedded multiplexed fibre-optic sensors, *Composite Structures* **66** 317–326.

7. Davis, M.A., Kersey, A D, Sirkis, J and Friebele, E J, 1996, Shape and vibration mode sensing using a fiber optic Bragg grating array, *Smart Mater. Struct.* **5** 759-765.
8. Bang, HJ., Kang, HK, Hong, CS and Kim, CG, 2005, Optical fiber sensor systems for simultaneous monitoring of strain and fractures in composites, *Smart Mater. Struct.* **14** N52–N58.
9. Kang, D.H., Kim, C.U. and Kim, C.G., 2006, The embedment of fiber Bragg grating sensors into filament wound pressure tanks considering multiplexing, *NDT&E International* **39** 109–116.
10. Chau, K., Moslehi, B., Song, G., and Sethi, V., "Experimental Demonstration of Fiber Bragg Grating Strain Sensors for Structural Vibration Control", *Proc. SPIE 5391, Sensors & Smart Structures Technologies for Civil, Mechanical, & Aerospace Systems* presented at *Smart Structures/NDE 2004*
11. Bocherens, E., Bourasseau, S., Dewynter-Marty, V., Py, S., Dupont, M, Ferdinand, P. and Berenger, H., 2000, Damage detection in a radome sandwich material with embedded fiber optic sensors, *Smart Mater. Struct.* **9** 310–315.
12. Takeda, N., 2002, Characterization of microscopic damage in composite laminates and real-time monitoring by embedded optical fiber sensors, *Int. Journal of Fatigue* 24 281–289.
13. Li, H.C.H., Herszberg, I., Mouritz, A.P., Davis, C.E., and Galea, S.C., 2004, Sensitivity of embedded fibre optic Bragg grating sensors to disbonds in bonded composite ship joints, *Composite Structures* **66** 239–248.
14. Fan, Y. and Kahrizi, M., 2005, Characterization of a FBG strain gage array embedded in composite structure, *Sensors and Actuators* A 121 297–305.
15. Takeda, N., Okabe, Y., Kuwahara, J., Kojima, S., and Ogisu, T., 2005, Development of smart composite structures with small-diameter fiber Bragg grating sensors for damage detection: Quantitative evaluation of delamination length in CFRP laminates using Lamb wave sensing, *Composites Science and Technology* 65 2575–2587.
16. Jung-Ryul Lee, J.R. and Tsuda, H., 2005, A novel fiber Bragg grating acoustic emission sensor head for mechanical tests, *Scripta Materialia* **53** 1181–1186.
17. Suresh, R., Tjin, S.C. and Ngo, N.Q., 2004, Shear force sensing by strain transformation using non-rectilinearly embedded fiber Bragg grating, *Sensors and Actuators* A 116 107–118.
18. Lestari, W., Qiao, P., and Hanagud, S., (2006). "Curvature Mode Shape-based Damage Assessment of Carbon/epoxy Composite Beams Using Piezoelectric Materials," *Journal of Intelligent Material Systems and Structures* **17**(7) in July issue.
19. Ratcliffe, C.P. and Bagaria, A., 1998, A vibration technique for locating delamination in a composite beam, *AIAA Journal* **36**(6) 1074-77.
20. Chang, F.K., "Structural health monitoring: a summary report", *Proc 2nd International Workshop on Structural Health Monitoring* (1999).
21. Hamey, C.S., Lestari, W., Qiao, P. and Song, G., "Experimental Damage Identification of Carbon/epoxy Composite Beams Using Curvature Mode Shapes", *Structural Health Monitoring: an International J.* (2004).
22. Ming-Gang Xu, Harold Geiger, Jean-Luc Archambault, Laurence Reekie, John P. Dakin, "Novel frequency-agile interrogating system for fiber Bragg grating sensors", *Proceedings SPIE* **2071**, pp. 59-65 (1993).
23. Jackson, D. A., Ribeiro, A. B. L., Reekie, L., Archambault, J. L., and Russell, P. St.: "Simultaneous interrogation of fibre optic grating sensors". *Proc. OFS'9*, Florence, pp. 43-46 (1993).
24. Davis, M. A., Kersey, A. D., Sirkis, J. and Friebele, E. J., "Shape and vibration mode sensing using a fiber optic Bragg grating array," *Smart Materials and Structures* **5**, 759-765 (1996).
25. Han, L., Voloshin, V. and Coulter, J., "Application of the integrating fiber optic sensor for vibration monitoring," *Smart Materials and Structures* **4**, 100-105 (1995).
26. Moslehi, B., Black, R.J., Toyama, K., Shaw, H.J., 'Multiplexible Fiber-Optic Strain Sensor System with Temperature Compensation Capability', U.S. Patent 6597822, issued July 22, 2003, U.S. Patent 6788835, issued Sept 7, 2004, and U.S. Patent 6895132, issued May 17, 2005.
27. Black, R.J., Chau, K., Good, L.K., Hernandez, M., Oblea, L., Moslehi, B., 'Fiber-Optic Sensing for Thermal Protection Structures in Vehicle Health Monitoring', *Proc. Quantitative Non Destructive Evaluation (QNDE),* 2005.
28. Black, R.J., Chau, K., Good, L.K., Moslehi, B., 'High-temperature fiber optic sensors for integrated systems health management', *Proc.17th Aeromat Conference & Exhibition (invited paper),* 2006.